



# Geant4 validation of neutron production on thick targets bombarded with 120 GeV protons



Mohammad S. Sabra

NASA Postdoctoral Program Fellow, Marshall Space Flight Center, Huntsville, AL 35805, USA

## ARTICLE INFO

### Article history:

Received 16 March 2015  
 Received in revised form 8 May 2015  
 Accepted 17 June 2015  
 Available online 10 July 2015

### Keywords:

Geant4  
 Proton reaction  
 Thick target  
 Neutron production

## ABSTRACT

Neutron energy spectra and angular distributions are calculated for 120 GeV protons on thick graphite, aluminum, copper, and tungsten targets using relevant physics models within the Monte-Carlo simulation package Geant4. The calculations are compared to data from recent experiment. Discrepancies are observed between experimental data and Geant4 models, and suggest that improvements of the intra-(INC) and inter-nuclear cascade processes employed by the models are required.

© 2015 Elsevier B.V. All rights reserved.

## 1. Introduction

High-energy protons and heavy-ions accelerated onto thick targets can produce large numbers of neutrons through spallation reactions [1–3]. When high-energy protons and heavy-ions impinge upon a thin target, they may have only one nuclear interaction take place, but thick targets are more likely to have multiple interactions. The energetic particles produced (nucleons, pions, kaons, etc.) can induce secondary reactions that produce additional neutrons. These processes are described by the intra- (INC) and inter-nuclear cascade processes [4,5]. Thus, the radiation shielding is essentially important to protect workers and nearby inhabitants from the penetrating neutrons produced in these reactions. To estimate source terms of the accelerator shielding design, energy spectra and angular distribution data of secondary neutrons from thick targets are indispensable. Such data are also crucial for estimating the induced activities and ambient dose equivalent behind the shielding walls of high-energy accelerators.

Monte-Carlo transport codes are a vital part of the design of shielding. They are used to estimate neutron productions, activities, and ambient dose equivalent. The predictions of these codes are verified by comparison with experimental data, if available, or other Monte-Carlo transport codes used as benchmark. Experimental data, however, make a good validation of these codes, and among the needed data, the energy and angular distributions of spallations produced neutrons. Recently, Kajimoto et al.

[6] have measured neutron energy spectra and angular distributions for 120 GeV protons on thick graphite, aluminum, copper, and tungsten targets. They have compared their measured data with the predictions of the parameterized three-moving-source model, as described in [6], as well as with the Monte-Carlo codes PHITS and FLUKA. Whereas the parameterization showed a good agreement with the measured data, both PHITS and FLUKA underestimated the measured data, in particular the high-energy part of the neutron energy spectra in the forward direction. This suggests that improvements of both models, PHITS and FLUKA, for thick targets are required, especially the intra/inter-nuclear cascade processes of the reaction, which are responsible for the high-energy part of the neutron spectra in the forward direction [7].

To test other transport codes used for shielding design, we have adopted the Monte-Carlo transport code Geant4, which simulates the propagation and interaction of particles with matter [8]. A very important feature of Geant4 is that it provides physics processes that cover a comprehensive set of particles and materials over a wide range of energy. The users have the complete freedom to choose those models that best match their needs.

Geant4 has been, and continues to be, tested and validated against many available experimental data on thin targets as well as on thick targets [9]. Thus, the availability of recent data from thick targets [6] is the motivation to test the intra/inter-nuclear cascade codes implemented within the Geant4 models. To fulfill our motivations, we have tested, in this work, the following Geant4 models (1) QGSP-BIC is the Quark-Gluon-String model (QGS) combined with the intra-nuclear cascade model BinaryCascade (BIC), and followed by the Pre-compound model

E-mail address: [mohammad.s.sabra@nasa.gov](mailto:mohammad.s.sabra@nasa.gov)

(P) which is used for de-excitation, (2) QGSP-BERT is the QGSP model combined with the intra-nuclear cascade model BertiniINC (BERT), (3) QGSP-INCLXX is the QGSP model combined with INCLXX (which is a modified version of the original Liège IntraNuclearCascade (INCL) model), and (4) SHIELDING model which is based on FTFP-BERT-HP model (Fritiof string model (FTF) combined with the BertiniINC (BERT) and Pre-compound model (P) using high precision (HP) neutron cross-section data).

In the following sections we describe the reaction mechanism and energy ranges of the models (Section 2), Geant4 simulation setup (Section 3), the simulation results compared with the experiment with discussion of the results (Section 4), and conclusions of this work (Section 5).

## 2. Geant4 nuclear physics models

The interaction of a proton with a nucleus is characterized by both fast and slow processes. The fast process, called the intra-nuclear (INC) cascade process, results in a highly excited nucleus which may decay by fission or pre-compound emission. The slower compound nucleus phase follows with evaporation. The cascade begins when an incident proton strikes a nucleon in the target nucleus and produces secondaries. The secondaries may, in turn, interact with other nucleons or be absorbed. The cascade ends when all particles escape the nucleus, if they are able to do so kinematically. At the end of the cascade, an excited fragment is formed for further treatment in pre-compound and nuclear de-excitation processes. Both processes, fast and slow, are employed by the Geant4 models under test. However, the energy range for each model is different. QGS model is valid at  $E \geq 20$  GeV, while both BIC and BertiniINC models are valid at  $E \leq 10$  GeV. To bridge the energy regions not covered by QGS and both BIC and BertiniINC, the Fritiof string model (FTF) is used, which is valid at  $E \geq 5$  GeV. INCLXX models is valid at  $E \leq 20$  GeV. SHIELDING model is valid at all energies since it is based on the FTFP-BERT-HP.

It is worth mentioning that the QGSP-INCLXX package is suitable for applications where spallation reactions are important, such as Accelerator-Driven Systems (ADS), and spallation targets (i.e. thick targets), while the SHIELDING model is recommended for shielding applications and space physics [10].

## 3. Geant4 simulation setup

To compare neutron spectra and angular distribution data [6] with Geant4 calculations, we have used the latest version of Geant4, version 10.01. In order to examine the ability of Geant4 models, all the calculations have been done with the actual thickness and dimensions of the targets as described in [6]. Ring-type detectors corresponding to the neutron detectors in the experiment were employed to gain the statistics for the number of emitted neutrons. The target was located at the center of a sphere depicted by the rings. The distance between the center of target and rings was set at 470 cm (which is the average distance for the 4 detectors used in the experiment [6]). A pencil beam of 120 GeV protons was incident upon the center of the target, and originates at a distance 1 mm from the left edge of the target (assuming the beam's direction is to the right in the +z-axis direction). The number of simulated events was  $1.0 \times 10^9$  events. For each neutron passing through the bounding sphere, the energy and angle relative to the beam were recorded. The simulation has been performed under a parallel computing environment.

## 4. Discussion and results

### 4.1. Neutron energy spectra and angular distributions

Calculations of Geant4 models for neutron energy spectra at angles  $30^\circ$ ,  $45^\circ$ ,  $120^\circ$ , and  $150^\circ$  for graphite, aluminum, copper, and tungsten targets bombarded with 120 GeV protons are shown in Fig. 1. The calculations are compared with the data [6]. The upper edge of the highest energy bin was 3000 MeV (the upper edge in the experiment).

In the forward directions ( $30^\circ$ ,  $45^\circ$ ), Geant4 models show reasonable agreement with the data at lower energies ( $E < 400$  MeV) compared to higher energies ( $E > 400$  MeV) where the models underestimate the data, especially for thicker and higher-Z targets. In the backward directions ( $120^\circ$ ,  $150^\circ$ ), the models show a general agreement with the data at  $E > 100$  MeV, while underestimate the data at  $E < 100$  MeV.

Fig. 2 shows Geant4 calculations of neutron angular distributions compared with the data [6]. The calculations are integrated between 25 MeV and 3000 MeV for each emission angle (as in the experiment). Geant4 models follow the trend of the data, yet they underestimate the data except for the graphite case at forward angles.

In the forward direction, production of high-energy neutrons is governed by the intra/inter-nuclear processes, while production of intermediate-energy neutrons is governed by the pre-equilibrium process. For thick targets, however, a high number of neutrons are produced due to multiple interactions (inter-nuclear process). The low neutron productions of Geant4 models at high energies suggest that improvements of the intra/inter-nuclear cascade processes for thick targets is required. On the other hand, agreements between the models and the data for the intermediate neutron energies suggest that the pre-equilibrium process is handled reasonably well for thick targets.

The situation is different in the backward direction, where production of neutrons is mainly governed by the pre-equilibrium process as well as the evaporation/fission processes. Experimentally, the lower energy limit of the neutron spectra was 25 MeV, which excludes most of the evaporative neutrons. This suggests that most of the neutrons measured in the backward direction are produced in the pre-equilibrium process, which starts when the intra/inter-nuclear cascade processes end. This suggests that improvements of the intra/inter-nuclear cascade processes will affect the pre-equilibrium process, and, as a whole, will have an impact on the number of neutrons produced.

For the angular distribution calculations, we have noticed that if we integrate the calculations between 5 MeV and 3000 MeV, which includes evaporative/fission neutrons, significant improvements in the calculations are observed, especially in the backward angles. This suggests that the measured data is a good validation for the intra/inter-nuclear and pre-equilibrium processes.

Overall, SHIELDING model shows the highest prediction power among Geant4 models while QGSP-INCLXX shows the lowest prediction power, and no significant difference between the prediction of QGSP-BIC and QGSP-BERT, since their intra-nuclear cascade processes are similar [10].

### 4.2. Number of neutrons

The low production of neutrons calculated by Geant4 was also noted by Araújo et al. [11] and Mario et al. [12], and to explain this phenomenon, Kajimoto et al. [6] suggested that the number of neutrons released from the target is determined by the following factors. (1) The reaction rate of the incident protons with the target

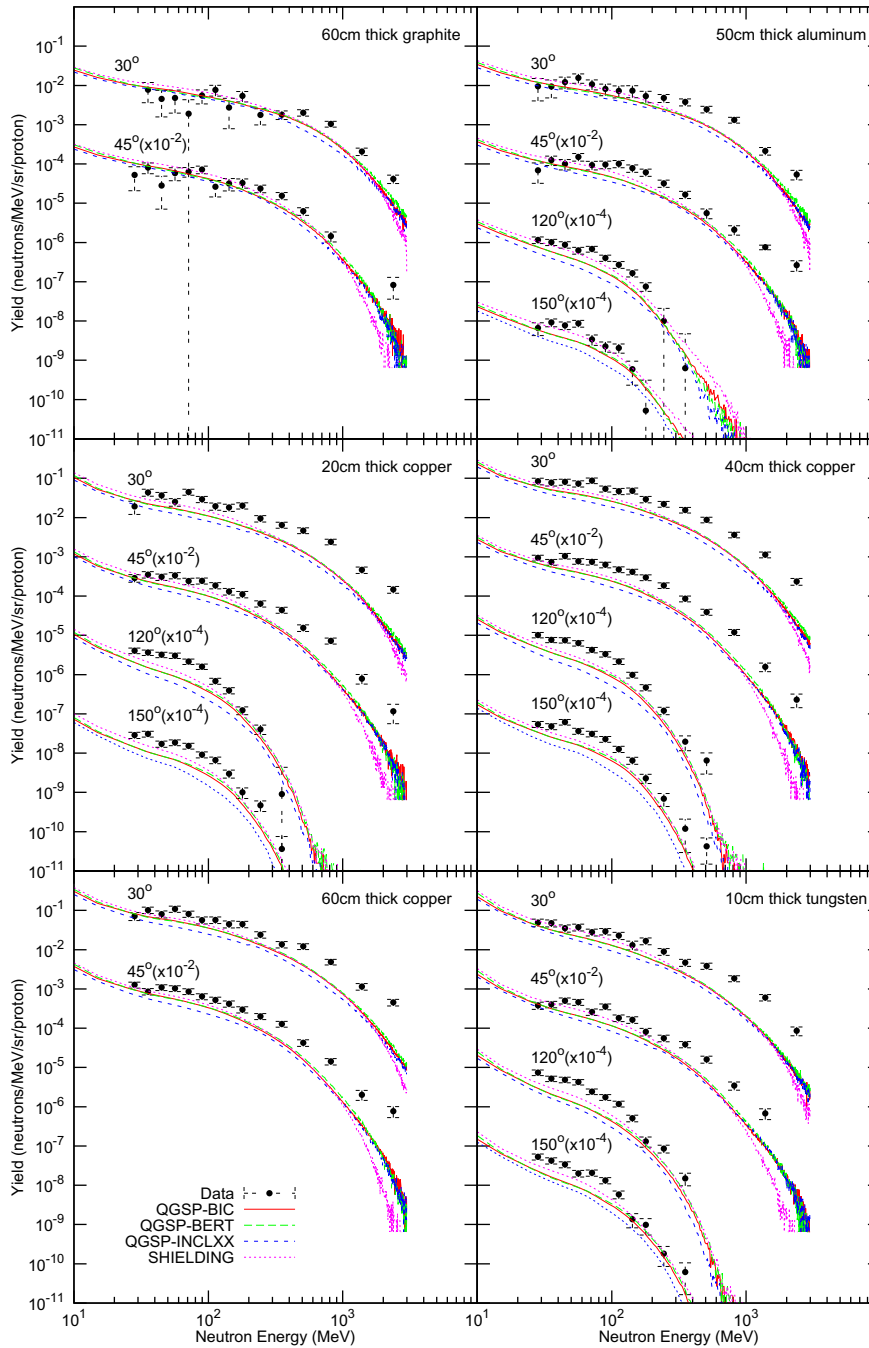


Fig. 1. Neutron energy spectra calculations compared with data from [6].

nuclei, (2) the development of the hadronic cascade, and (2) the number of neutrons produced by the interaction.

For factor (1), we have calculated the reaction rate for Geant4 using the following relation

$$R = 1 - e^{-n\sigma_t t} \quad (1)$$

where  $n$  is number density of the target,  $\sigma_t$  is the hadronic total cross-section of 120 GeV protons for each target, and  $t$  is the thickness of the target. Table 1 summarizes the Geant4 hadronic total cross-section and the corresponding reaction rate compared with PHITS calculations from [6]. The relative difference in the reaction rate of Geant4 compared to PHITS is less than 3% except for the tungsten target which is about 8%. Thus, both codes provide similar reaction rate, which is also consistent with the experimental

hadronic total cross-section reported in [6]. This suggests that the number of neutrons produced by Geant4 is not affected by its reaction rate.

For factor (2), we compare the neutron emission probability ratio between thin target and thick target of the same material bombarded by the same incident particle at the same energy. Such a ratio is important when trying to determine the source of discrepancy between simulated results and experimental data. For example, equivalent ratios between simulated and experimental data for thin and thick targets would suggest that the development of the hadronic cascade processes are handled adequately within the simulation. Table 2 summarizes Geant4 calculations of Neutron Emission Probability (NEP) from the target to reaction rate (R) (from Table 1) for copper of various thicknesses normalized to

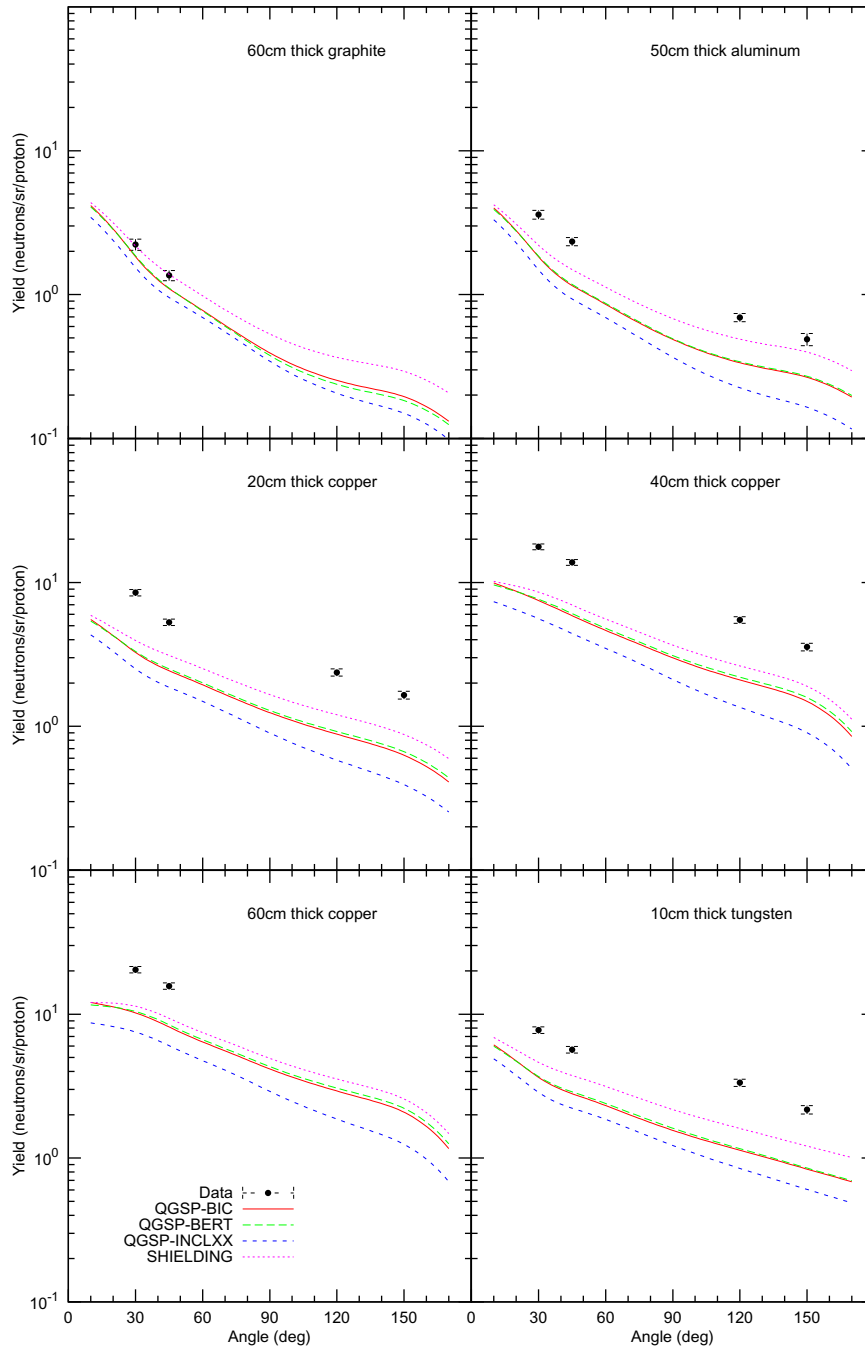


Fig. 2. Neutron angular distribution calculations compared with data from [6].

**Table 1**  
Hadronic total cross-section and reaction rate.

Target	$\sigma_t(b)$		Reaction rate	
	Geant4	PHITS <sup>a</sup>	Geant4	PHITS <sup>a</sup>
C (60 cm)	0.330	0.336	0.815	0.839
Al (50 cm)	0.646	0.649	0.857	0.858
Cu (20 cm)	1.341	1.290	0.897	0.888
Cu (40 cm)	1.341	1.290	0.989	0.987
Cu (60 cm)	1.341	1.290	0.999	0.999
W (10 cm)	3.494	2.910	0.890	0.822

<sup>a</sup> From Ref. [6].

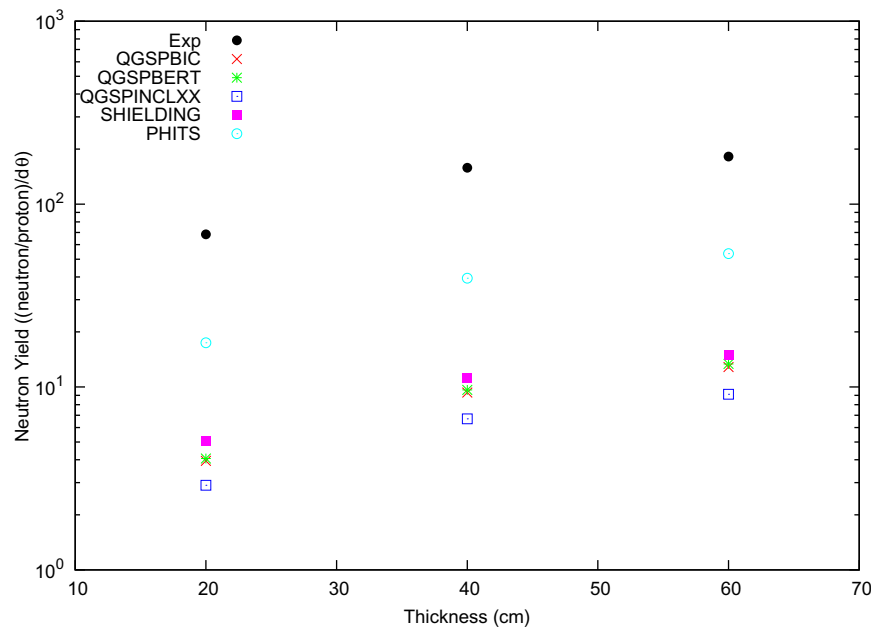
the 20 cm-thick copper. The table also shows the experimental data and PHITS results from [6] for comparison.

Although the ratio increases with target thickness, discrepancy between Geant4 calculations and the data is obvious for the very forward angle (30°) (25–45%), where the intra/inter-nuclear cascade process dominates. As the angle increases, Geant4 reasonably agrees with the data (~10%), which suggests that the pre-equilibrium processes (dominating in the backward directions) are handled adequately within the Geant4 models. We also note a discrepancy between Geant4 models and PHITS at 30°, though both agree in the reaction rate calculations. The reason PHITS has a higher ratio is because of the inclusion of evaporative/fission neutrons in the calculations (where a cut-off energy of

**Table 2**

Ratio of neutron emission probability to reaction rate (NEPR) for copper of various thicknesses normalized to the 20 cm-thick copper.

$\theta$ (deg)	$t$ (cm)	Exp <sup>a</sup>	QGSP-BIC	QGSP-BERT	QGSP-INCLXX	SHIELDING	PHITS <sup>a</sup>
30	20	1.00	1.00	1.00	1.00	1.00	1.00
	40	1.87 ± 0.13	1.48	1.49	1.44	1.40	2.00
	60	2.14 ± 0.15	1.63	1.65	1.56	1.50	2.67
45	20	1.00	1.00	1.00	1.00	1.00	1.00
	40	2.34 ± 0.16	2.17	2.18	2.12	2.02	2.05
	60	2.64 ± 0.19	2.96	2.99	2.87	2.68	2.76
120	20	1.00	1.00	1.00	1.00	1.00	1.00
	40	2.09 ± 0.16	2.16	2.17	2.11	1.99	2.04
150	20	1.00	1.00	1.00	1.00	1.00	1.00
	40	1.93 ± 0.17	2.14	2.16	2.08	1.97	2.03

<sup>a</sup> From Ref. [6].**Fig. 3.** Neutron yield for 120 GeV proton on copper of various thicknesses.

5 MeV was used for PHITS and FLUKA calculations [6]). Thus, the very forward direction, where the intra/inter-nuclear process dominates, is enhanced by the addition of the evaporative neutrons. As the angle increases, the intra/inter-nuclear neutron component diminishes while the evaporative/fissional components increase.

For factor (3), to investigate the number of neutrons factor, it is more appropriate to investigate the mean number of neutrons emitted per incident proton which is known as the neutron multiplicity distribution. Since the experiment [6] was not designed to measure neutron multiplicity distribution, we can observe a similar distribution if we compare neutron yield for copper at various thicknesses. To achieve this, we have calculated the total neutron production (neutron yield) in units of ((neutron/proton)/ $d\theta$ ), where  $d\theta$  is the angular width, by integrating the angular distributions at 30°, 40°, 120°, and 150° for copper of various thicknesses for each Geant4 model as well as for PHITS and the experiment. For 60 cm-thick copper, data is only available for 30°, and 45°. Using the fact that the neutron yield per incident proton attains a maximum value due to increase of the reaction rate [5,13], we expect that the angular distributions for both 40 cm-thick copper and 60 cm-thick copper are similar when normalized at 30°. Thus, by normalizing the angular distribution for 40 cm-thick copper to that of 60 cm-thick copper, we extrapolated the angular distribution for 60 cm-thick copper at 120° and 150°, and calculated the neutron

yield. Fig. 3 shows the calculated neutron yield for copper at various thicknesses for Geant4 models, the experiment, and PHITS. Geant4 models show lower neutron yield compared to the data by more than one order of magnitude, and for various thicknesses of copper. This suggests that the number of neutrons from the interaction is the main cause of the low production of neutrons by Geant4 models, which depends on the intra/inter-nuclear cascade processes handled by Geant4 models. On the other hand, PHITS shows higher neutron yield compared to Geant4 models, since lower cut-off energy (5 MeV) is used in PHITS calculations of angular distributions.

The issue of producing low number of neutrons by Geant4 models, as well as PHITS and FLUKA, is complicated. However, to help understanding the issue in more depth, two more tests need to be investigated. Firstly, for thick targets most of the high-energy neutrons are produced in reactions induced by secondary particles. Thus, investigating the relative contribution of individual processes (photo-nuclear, muon and pion spallations, proton spallation, deuteron break-up, etc.) to the total neutron yield will assist in identifying the issue of low neutron production [11]. Secondly, thick target experiments are also interested in measuring neutron multiplicity distribution, and validations of Geant4 models against experimental data for neutron multiplicity distributions will also assist in improving Geant4 models for thick targets.

## 5. Conclusion

Neutron energy spectra and angular distributions from thick graphite, aluminum, copper, and tungsten bombarded by 120 GeV protons are calculated using Geant4 physics models QGSP-BIC, QGSP-BERT, QGSP-INCLXX, and SHIELDING. When compared with experiment, the calculations underestimated the data. Total neutron production yield for Geant4 models is lower than the experiment by more than one order of magnitude. This suggests that improvements of the intra/inter-nuclear cascade processes handled by Geant4 models for thick targets are required. Investigation of the contributions of individual reaction processes to the total neutron yield as well as neutron multiplicity distributions will assist in identifying the cause of the low neutron production in Geant4 simulations.

## Acknowledgments

The author would like to thank Dr.Kajimoto for providing us with the experimental data in numerical form. This work was

supported by an appointment to the NASA Postdoctoral Program at Marshall Space Flight Center, administered by Oak Ridge Associated Universities through a contract with NASA.

## References

- [1] T. Kurosawa, N. Nakao, T. Nakamura, et al., *Phys. Rev. C* 62 (2000) 044615.
- [2] S. Leray, F. Borne, S. Crespin, et al., *Phys. Rev. C* 65 (2002) 044621.
- [3] D. Satoh, D. Moriguchi, T. Kajimoto, et al., *Nucl. Instr. Methods B* 644 (2011) 59.
- [4] K. Borekov, A. Kaidalov, S. Kiselev, N.Y. Smorodinskaya, *Sov. J. Nucl. Phys.* 55 (1992) 936.
- [5] L. Pienkowski, F. Goldenbaum, D. Hilscher, U. Jahnke, J. Galin, B. Lott, *Phys. Rev. C* 56 (1997) 1909.
- [6] T. Kajimoto, N. Shigyo, T. Sanami, et al., *Nucl. Instr. Methods B* 337 (2014) 68.
- [7] A. Dar, J. Vary, *Phys. Rev. D* 6 (1972) 2412.
- [8] S. Agostinelli, J. Allison, K. Amako, et al., *Nucl. Instr. Methods A* 506 (2003) 250.
- [9] Validation of Geant4. <<http://geant4.cern.ch/results/index.shtml>>.
- [10] Geant4 Physics Reference Manual, <<http://geant4.cern.ch/support/userdocuments.shtml>>.
- [11] H.M. Araújo, V.A. Kudryavtsev, N.J.C. Spooner, T.J. Summer, *Nucl. Instr. Methods A* 545 (2005) 398.
- [12] M.G. Marino, J.A. Detwiler, R. Henning, R.A. Johnson, A.G. Schubert, J.F. Wilkerson, *Nucl. Instr. Methods A* 582 (2007) 611.
- [13] B. Lott, F. Cnigniet, et al., *Nucl. Instr. Methods A* 414 (1998) 117.